Agriculture and Food

AIMS Agriculture and Food 11(3): 820–846.
DOI: 10.3934/agrfood.2026041
Received: 29 May 2026
Revised: 04 September 2026
Accepted: 16 September 2026
Published: 30 September 2026

https://www.aimspress.com/journal/agriculture

Research article

Hyperspectral analysis of sugar beet (*Beta vulgaris* L.) response to different potassium fertilization levels for sustainable crop production

Ghada A. Khdery[1,*], I. M. El-Metwally[2,*], Nazih Y. Rebouh[3], Oybek Fayziev[4] and Mohamed S. Shokr[3,5]

[1] National Authority for Remote Sensing and Space Sciences (NARSS), Cairo 11843, Egypt
[2] Botany Department, National Research Centre, P.O. Box 12622, Dokki, El–Behos St. Dokki, Cairo, Egypt
[3] Department of Environmental Management, Institute of Environmental Engineering, RUDN University, 6 Miklukho-Maklaya Street, 117198 Moscow, Russia
[4] Department of Digital Technologies, Alfraganus University, Tashkent, Uzbekistan
[5] Soil and Water Department, Faculty of Agriculture, Tanta University, Tanta 31527, Egypt

* **Correspondence:** Email: ghada.ali@narss.sci.eg; im_elmetwally@yahoo.com.

Abstract: Sugar beet is an economically important crop, and optimizing potassium (K) fertilization is essential for improving productivity, particularly in sandy soils. In this study, we evaluated the effects of five potassium rates (0, 39.5, 79.1, 118.6, and 158.1 kg K ha^{-1}) on sugar beet (Beta vulgaris L.) growth, yield, and canopy spectral response under field conditions. Two consecutive seasons (2023/2024 and 2024/2025) were conducted at the National Research Centre experimental farm, El-Behaira, Egypt, using a randomized complete block design with three replicates. Canopy reflectance (350–1100 nm) was measured using an ASD FieldSpec, and vegetation indices (NDVI, CRI1, ARI1, PSRI, and SIPI) were derived to characterize plant physiological status. Potassium application significantly improved agronomic traits and spectral indicators compared with the control, with 118.6 kg K ha^{-1} providing the most consistent and efficient response across seasons. By improving yield stability and nutrient use efficiency, the proposed potassium management strategy contributes to improving sugar beet productivity and nutrient management efficiency under arid and semi-arid conditions. The combined use of field spectroscopy and conventional growth measurements offers a practical approach for identifying suitable potassium rates and supporting more efficient nutrient management in sandy soil environments.

Keywords: sugar beet; potassium fertilizer; hyperspectral sensing; spectral indices; precision agriculture; remote sensing; ASD FieldSpec

1. Introduction

Sugar beet is considered one of the most economically significant sugar-producing crops worldwide, ranking the second after sugarcane in terms of global sugar output [1–3]. According to the most recent FAO dataset, global sugar beet production reached approximately 280 million tonnes in 2023 under cultivation areas of roughly 4.4 to 4.6 million hectares [4,5]. The Russian Federation leads global production with approximately 55 million metric tons, followed by France, the United States, Germany, and Turkey [6].

Sugar beet (*Beta vulgaris* L.) is a temperate-region crop of global importance, serving as the second-largest source of sugar after sugarcane (*Saccharum officinarum* L.) [2]. It accounts for approximately 30% of global sugar consumption [7], primarily due to the high sucrose concentration stored in its roots [8].

Sugar beet, a member of the *Chenopodiaceae* family, is primarily cultivated in temperate and subtropical regions due to its specific soil and climatic requirements. In Egypt, the crop is particularly well-suited for cultivation given its notable tolerance to salinity and arid desert environments, positioning it as a key alternative to sugarcane in narrowing the gap between local sugar production and consumption. While sugarcane dominates the agricultural landscape in Upper Egypt, sugar beet is predominantly grown under irrigated systems in the Nile Delta and reclaimed lands. Moreover, sugar beet contributes approximately 1.05 million tons of sugar annually, representing 45.55% of Egypt's total domestic sugar output. In response to increasing demand, the Egyptian government has implemented a range of strategies aimed at enhancing the quantity and quality of sugar production [9].

In Egyptian agro-ecosystems, sugar beet is frequently cultivated under conditions characterized by multiple abiotic constraints, including soil salinity, limited water availability, and nutrient imbalances. These stress factors can strongly influence physiological performance, sucrose accumulation, and overall crop productivity, underscoring the importance of optimized nutrient management, particularly potassium fertilization, under such challenging environments.

Under sandy soil conditions typical of newly reclaimed lands in Egypt, potassium availability is often limited by low cation exchange capacity and high leaching losses. Consequently, inappropriate potassium management can lead not only to yield reduction but also to inefficient fertilizer use and increased production costs. Identifying potassium rates that balance crop performance and input efficiency therefore represents a practical challenge for sugar beet production systems in arid environments.

From a physiological perspective, sugar beet roots serve as a major raw material in white sugar production. While the crop is mainly composed of carbon, hydrogen, and oxygen, other essential elements are required for its structural and biochemical processes [10]. Macronutrients such as nitrogen (N), phosphorus (P), sulfur (S), potassium (K), calcium (Ca), and magnesium (Mg) are needed in relatively large quantities, whereas micronutrients like boron (B), copper (Cu), iron (Fe), manganese (Mn), molybdenum (Mo), and zinc (Zn) are required in smaller amounts. Among these, potassium is particularly critical, as sugar beet is considered a potassium-demanding crop [11].

Potassium plays a multifaceted role in plant growth and development. It enhances nutrient uptake, activates enzyme systems, supports osmotic regulation, and facilitates stomatal functioning, contributing to cellular metabolism and stress tolerance [12]. In many crops, enhanced potassium availability is strongly correlated with improved physiological traits, including higher chlorophyll concentration, greater biomass accumulation, and increased yield. Potassium regulates stomatal conductance, osmotic balance, and enzyme activation, all of which directly influence photosynthetic efficiency and pigment stability. These physiological improvements are typically reflected in spectral behavior, particularly within chlorophyll-sensitive vegetation indices, making hyperspectral sensing an effective tool for detecting plant responses to potassium nutrition. For instance, spraying 600 mg L^{-1} of nano-K on *Ocimum basilicum* increased leaf area, biomass, grain yield, and chlorophyll content [13]. Likewise, Zangeneh, Nayereh [14] reported that nano-K at 1000 mg L^{-1} increased chlorophyll content, while 2000 mg L^{-1} enhanced potassium content and enzyme activity in grapevines. Under drought conditions, foliar application of K_2SO_4 at 200 mg L^{-1} improved growth parameters, pigment content, and stomatal opening in wheat [15]. [16] also observed enhanced maize yield when plants were treated with 500 mg L^{-1} of nano-potassium combined with 150 kg ha^{-1} of potassium sulfate.

In sugar beet, potassium fertilization has been found to boost root development and increase sucrose concentration [17]. While researchers have investigated nitrogen and phosphorus fertilization, fewer have focused on potassium despite its vital role in stress tolerance, enzyme activation, and osmotic adjustment. A field study by [18] revealed that applying 177.9 kg K ha^{-1} significantly increased N, P, and K content in roots, alongside improvements in root yield, sucrose percentage, and juice purity. However, optimal application rates under sandy soil conditions remain unclear. Despite the recognized importance of potassium nutrition in sugar beet, field-based studies that simultaneously evaluate agronomic performance and plant spectral response under sandy soil conditions remain limited. In particular, there is insufficient evidence on how different potassium rates influence canopy reflectance behavior and vegetation indices under practical field management. With advancements in technology, remote sensing has evolved as a powerful non-destructive method for agricultural monitoring. While originally used in Earth and climate sciences, remote sensing and geospatial approaches have expanded to environmental and agricultural applications [19]. Remote sensing has been widely applied for monitoring crop nitrogen and water stress, plant physiological responses, and irrigation-related stress [20–23]. Spectral and geospatial approaches have also been used for evaluating irrigation and nitrogen conditions and other environmental applications [24–26]. In addition, remote sensing has supported water-stress detection, nitrogen assessment, and crop growth and yield monitoring [27–29]. Early remote sensing research in Japan explored the use of red (650 nm) and near-infrared (850 nm) reflectance to estimate sugar beet root yield under different fertilization regimes [30]. The derived K-value from these bands proved to be a reliable yield predictor during the growing season, especially in August.

Subsequent studies extended remote sensing applications to nutrient deficiency diagnostics, particularly for nitrogen and phosphorus. By the 1990s, satellite-based imagery, notably Landsat TM, was used to estimate root sugar concentration and nitrogen uptake across sugar beet fields [29]. These studies demonstrated the utility of remote sensing in evaluating both yield and quality, aiding in precise fertilizer management.

Advances in hyperspectral sensing have enabled precise detection of physiological changes in crops through spectral reflectance patterns. In sugar beet, variations in reflectance, particularly in the blue and near-infrared regions, have been linked to changes in pigment content and tissue structure

under stress conditions. Prior work confirmed that these spectral zones are highly responsive to plant status, supporting the use of hyperspectral indices in assessing nutrient-related stress, such as potassium deficiency, during critical growth stages [31]. However, most remote sensing applications in sugar beet have concentrated on nitrogen or phosphorus deficiencies [32], with limited research addressing potassium fertilization. This knowledge gap is especially critical for arid and semi-arid regions like Egypt, where nutrient mismanagement can severely constrain productivity.

Further work linked satellite data with soil characteristics to explain spatial variability in yield. For example, low-yielding zones were associated with poor soil drainage, compact subsoil layers, and the absence of gravel strata [33]. On a broader scale, the integration of remote sensing with crop models like SUCROS enabled spatial yield prediction across large-scale agricultural regions [34,35].

Studies have confirmed the potential of remote sensing data acquired in summer to forecast final yield. In addition, hyperspectral data analytics enabled early identification and classification of potassium deficiency in crops before visible symptoms appear, thereby supporting improved management decisions. These documented correlations between spectral indices and potassium nutrient status strengthen the theoretical rationale for employing hyperspectral vegetation indices as indicators of plant performance and nutrient-fertilizer responses under different nutrient management regimes [32].

Linking conventional growth and yield measurements with spectral indicators may provide a practical decision-support tool for optimizing potassium fertilization, especially in environments where soil variability and nutrient losses complicate fertilizer management.

Our objective of this study was to evaluate the effects of different potassium fertilization rates on sugar beet growth, yield, and canopy spectral reflectance under field conditions. Field-based studies integrating agronomic performance with hyperspectral responses to graded potassium application under sandy-soil conditions remain limited. Therefore, by integrating conventional growth and yield measurements with hyperspectral reflectance and vegetation indices, we provide a framework for evaluating the agronomic and spectral responses of sugar beet to K nutrition and identifying an efficient potassium application rate for sandy soils. We hypothesized that increasing potassium fertilization rates would produce measurable changes in sugar beet growth, yield, canopy reflectance, and vegetation indices, enabling hyperspectral sensing to discriminate among potassium fertilization levels and identify the most efficient treatment under sandy-soil conditions.

2. Materials and methods

2.1. Study area

The field trials were carried out in Nubaria region, El-Behaira Governorate, Egypt (30°30′01.4″ N, 30°19′10.9″ E), over two seasons (2023/2024 and 2024/2025).

Comprehensive soil physical and chemical analyses were performed before sowing in both seasons to establish the baseline fertility of the site (Table 1). The soil was sandy in texture, with very low organic matter (0.6–0.8%), alkaline pH (8.31–8.63), and low available potassium (0.23–0.33 mmolc L^{-1}). Other soluble cations (Ca^{2+}, Mg^{2+}, Na^{+}) and anions (Cl^{-}, SO_4^{2-}, HCO_3^{-}) were also quantified. The baseline soil properties confirmed that observed differences among treatments were attributable to potassium fertilization rather than inherent soil variability (Figure 1).

Table 1. Physical and chemical analysis of the experimental soil in 2023/2024 and 2024/2025 seasons.

Soil characteristics	Values	
	Season 2023/2024	Season 2024/ 2025
Particle size distribution (%)		
Sand	91.30	88.67
Silt	0.75	0.93
Clay	7.89	10.30
Texture type	Sandy	Sandy
Chemical analysis		
O.M %	0.8	0.6
pH	8.57	8.63
EC (dS m^{-1})	0.3	3.3
Soluble cations (mmolc L^{-1})		
Ca++	1.5	1.48
Mg++	1.0	0.91
Na+	3.45	3.20
K+	0.33	0.23
Soluble anions (mmolc L^{-1})		
HCO_3^-	0.7	0.5
Cl^-	4.50	4.00
SO_4^{2-}	0.83	12.7

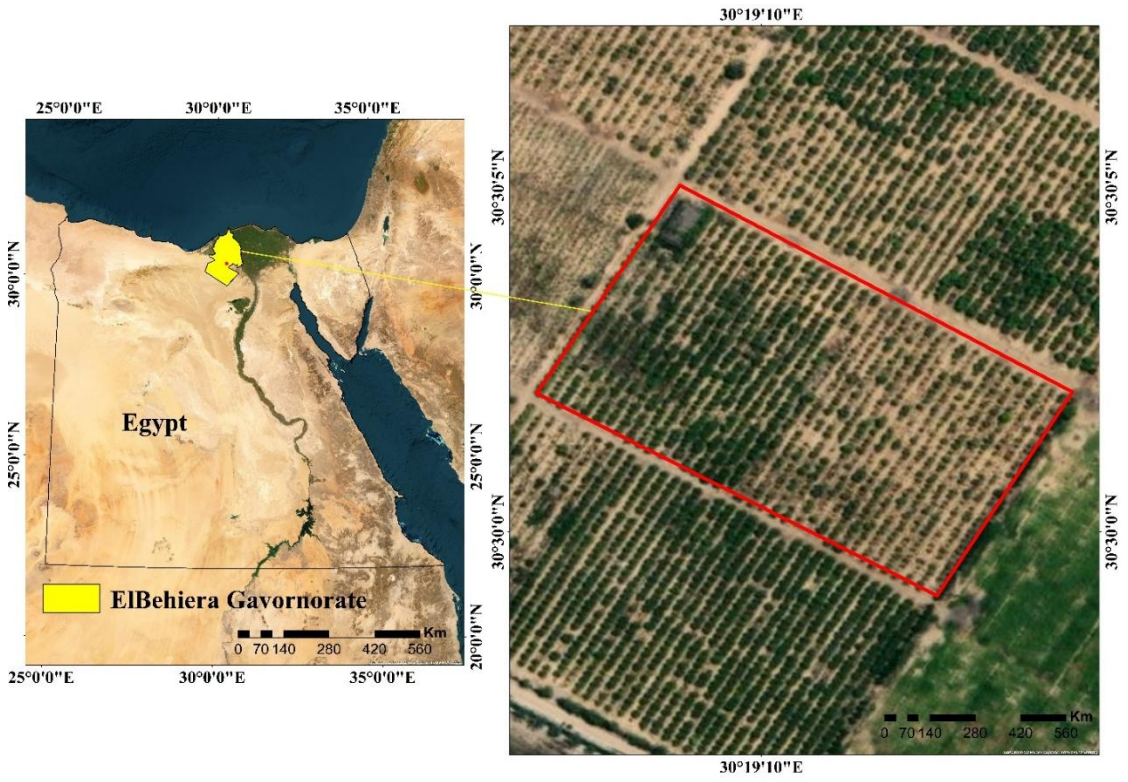


Figure 1. Location Map of the study area at the National Research Centre Experimental Farm, El-Behaira, Egypt.

2.2. Experimental design and potassium treatments

The experiments followed a randomized complete block design (RCBD) with five elemental potassium application rates: 0, 39.5, 79.1, 118.6, and 158.1 kg K ha^{-1}, each replicated three times. The original graphical treatment codes $0K_2O$, $20K_2O$, $40K_2O$, $60K_2O$, and $80K_2O$, retained in Figures 2–7, corresponded to 0, 39.5, 79.1, 118.6, and 158.1 kg elemental K ha^{-1}, respectively. Potassium was supplied as potassium sulfate containing approximately 39.8% elemental K and was applied in three equal splits at 50, 75, and 100 days after sowing (DAS). All physiological and spectral measurements at 120 DAS were taken approximately 20 days after the final potassium application to avoid any immediate short-term effects of fertilization on plant responses.

2.3. Crop establishment and cultural practices

Sugar beet (*Beta vulgaris* L., cv. Baraka), a monogerm variety obtained from the Sugar Crops Research Institute (Agricultural Research Center, Egypt), was manually sown in the third week of November in both seasons. Nitrogen fertilizer was applied at 178.6 kg N ha^{-1} as ammonium nitrate (33.5% N), while phosphorus was applied at 73.8 kg P_2O_5 ha^{-1} as ordinary superphosphate (15.5% P_2O_5). Potassium was supplied as potassium sulfate (48% K_2O) and applied in three equal splits at 50, 75, and 100 days after sowing (DAS). Potassium fertilizer was manually applied along the drip irrigation lines during routine field management practices. Plants were irrigated using a drip irrigation system based on crop water requirements. Weed control was performed manually, and pest management followed integrated pest management (IPM) practices.

2.4. Sampling strategy and plant measurements

Plant samples were collected at three stages according to the measurements taken during the experiment. SPAD chlorophyll readings were recorded at 90 DAS, while growth measurements were carried out at 120 DAS, representing the peak vegetative stage. Final yield and root characteristics were evaluated at harvest (180 DAS). From each experimental unit, ten representative plants were randomly selected for destructive measurements, giving a total of 150 plants per stage (10 plants × 3 replicates × 5 treatments). The measured traits included root length and diameter (cm), root and shoot fresh weight (kg $plant^{-1}$), shoot dry weight (kg $plant^{-1}$), SPAD chlorophyll values, and total root yield (kg m^{-2}).

2.5. Spectral data collection and indices calculation

Spectral reflectance of sugar beet leaves and the soil surface was measured using an ASD FieldSpec® 4 spectroradiometer. The spectroradiometer covered the full range of the visible to near-infrared spectrum (350–1100 nm), with a spectral resolution of 1.4 nm in the 350–1050 nm range. The instrument was positioned at a height of 1 m above the canopy and maintained at a nadir angle to capture accurate reflectance profiles. Raw DN values were calibrated using a Spectralon white reference and dark current correction, and then converted to reflectance (0–1). Figures display reflectance values consistently on the y-axis.

At each sampling stage (120 DAS for peak vegetative growth and 180 DAS for harvest), spectral readings were collected from ten representative plants per plot, giving a total of 150 plants per stage across all treatments (5 potassium levels × 3 replicates × 10 plants). To minimize soil background interference during canopy reflectance measurements, spectral scans were collected over fully developed sugar beet canopies with minimal visible soil exposure. The sensor field of view was maintained directly above the canopy at nadir position, and measurements were acquired under stable illumination conditions to reduce variability associated with soil reflectance and shadow effects.

Several vegetation indices were derived from spectral reflectance values to evaluate plant physiological status and nutrient response (Table 2). The following indices were computed using reflectance data from specified wavelengths:

Table 2. Summary of vegetation indices, algorithms, and sources. R_x is the reflectance at the given wavelength (nm).

Category	Index	Formula	Explanation	Ref.
Dry or senescent carbon	Plant Senescence Reflectance Index	PSRI = (R680 − R500)/R750	Chlorophyll carotenoids ratio	[36]
Broadband greenness	Normalized Difference Vegetation Index	NDVI = (R800 − R680)/(R800 + R680)	Biomass content	[37–39]
Leaf pigments	Anthocyanin reflectance index	ARI1 = 1/R550 − 1/R700	Anthocyanin amount	[40]
	Carotenoids Reflection index	CRI1 = (1/R510) – (1/R550)	Carotenoids/ chlorophyll ratio	[41]
	Structure Insensitive Pigment	SIPI = R800 − R440/R800 − R680	Carotenoids to chlorophyll in plant leaves	[42]

2.6. Soil reflectance and sampling

Soil spectral reflectance was also measured from surface samples of each treatment plot. Samples were air-dried and scanned under laboratory conditions using the same spectroradiometer, focusing on visible-NIR wavelengths. Baseline soil analyses confirmed that the experimental field was sandy with low organic matter and low available potassium across all plots (Table 1), ensuring that treatment differences could be attributed to applied potassium fertilization rather than soil heterogeneity.

2.7. Statistical analysis

All statistical analyses were conducted using JMP® Pro software. Data from each growing season were analyzed according to a randomized complete block design (RCBD) with three replicates. Analysis of variance (ANOVA) was performed separately for each growing season, and potassium treatment means for agronomic traits were compared using the least significant difference (LSD) test at $P \leq 0.05$. For between-season comparisons of the agronomic traits presented in Tables 3, 5, and 7, the residual error variance for each season was derived from the corresponding LSD value and the experimental design. The standard error of the difference between corresponding treatment means of

the two seasons was then calculated, and between-season differences were tested at $P \leq 0.05$ using the appropriate degrees of freedom. For spectral reflectance data, Tukey–Kramer HSD multiple-comparison tests were used to compare treatment means among spectral bands. Spectral vegetation indices (NDVI, CRI1, ARI1, PSRI, and SIPI) were calculated from reflectance measurements and used to support treatment comparisons.

3. Results

3.1. The effect of potassium fertilization levels on sugar beet plants at the growth stage (BBCH 49–51; 120 DAS)

The results in Table 3 illustrate the influence of potassium fertilization levels on sugar beet morphological traits after 120 days from sowing over two growing seasons. Root length exhibited a steady increase with increasing potassium application, reaching the highest values under 158.1 kg K ha^{-1} (19.50 cm in 2024/2025 and 22.55 cm in 2023/2024), compared to the control (16.60 cm and 16.23 cm, respectively). Similarly, root fresh weight rose progressively with higher potassium rates, peaking at 0.591 kg $plant^{-1}$ (2024/2025) and 0.461 kg $plant^{-1}$ (2023/2024) under the 158.1 kg K ha^{-1} treatment.

The results presented in Table 3 demonstrate a clear and progressive enhancement in sugar beet growth with increasing potassium application rates after 120 days from sowing. Shoot fresh weight exhibited a consistent upward trend, reaching its highest values under the 158.1 kg K ha^{-1} treatment (0.702 kg $plant^{-1}$ in 2024/2025 and 0.602 kg $plant^{-1}$ in 2023/2024), while the control treatment recorded the lowest biomass accumulation. Although both 118.6 and 158.1 kg K ha^{-1} resulted in substantial improvements in biomass production, the difference between these two rates remained relatively small, indicating that 118.6 kg K ha^{-1} may represent the most efficient rate from agronomic and economic perspectives.

Table 3. Effect of potassium fertilization levels on growth sugar beet plants after 120 days from sowing.

K application rate (kg K ha^{-1})	Shoot fresh weight (kg $plant^{-1}$) 2023/2024	2024/2025	Root fresh weight (kg $plant^{-1}$) 2023/2024	2024/2025	Root length (cm) 2023/2024	2024/2025
Control	0.429 c*	0.515 d*	0.335 c*	0.452 d*	16.23 e	16.60 d
39.5	0.530 b*	0.569 c*	0.380 b*	0.485 c*	18.31 d*	17.25 cd*
79.1	0.551 b*	0.625 b*	0.400 b*	0.520 b*	19.59 c*	17.88 c*
118.6	0.578 a*	0.675 a*	0.441 a*	0.570 a*	21.41 b*	18.68 b*
158.1	0.602 a*	0.702 a*	0.461 a*	0.591 a*	22.55 a*	19.50 a*
LSD 5%	0.025	0.028	0.033	0.027	1.12	0.78

Means followed by different lowercase letters within the same season are significantly different according to the LSD test at $P \leq 0.05$. An asterisk (*) indicates a significant difference between the two growing seasons for the same potassium treatment at $P \leq 0.05$. Values without an asterisk are not significantly different between seasons.

3.1.1. Spectral reflectance patterns of sugar beet under different potassium treatments

Figure 2 illustrates the reflectance behavior of sugar beet leaves under different potassium levels, showing a typical vegetation spectral signature. All treatments exhibited pronounced absorption features at approximately 450 nm (blue region) and 680 nm (red region), which correspond to chlorophyll pigment absorption, along with a distinct reflectance peak around 550 nm (green). Beyond 700 nm, a sharp rise along the red-edge region was observed, continuing into the near-infrared (NIR) region (750–850 nm).

The 118.6 kg K ha^{-1} and 158.1 kg K ha^{-1} treatments consistently produced the highest NIR reflectance, reflecting improved internal leaf structure, greater mesophyll density, and enhanced chlorophyll content. By contrast, the control and 39.5 kg K ha^{-1} treatments exhibited comparatively lower reflectance values, indicating reduced photosynthetic capacity and lower canopy vigor. Although 158.1 kg K ha^{-1} showed slightly higher NIR reflectance than 118.6 kg K ha^{-1}, the 118.6 kg K ha^{-1} treatment demonstrated a more stable and balanced spectral profile across the visible and NIR ranges. This pattern suggests that 118.6 kg K ha^{-1} treatment supports optimal physiological performance under sandy-soil conditions.

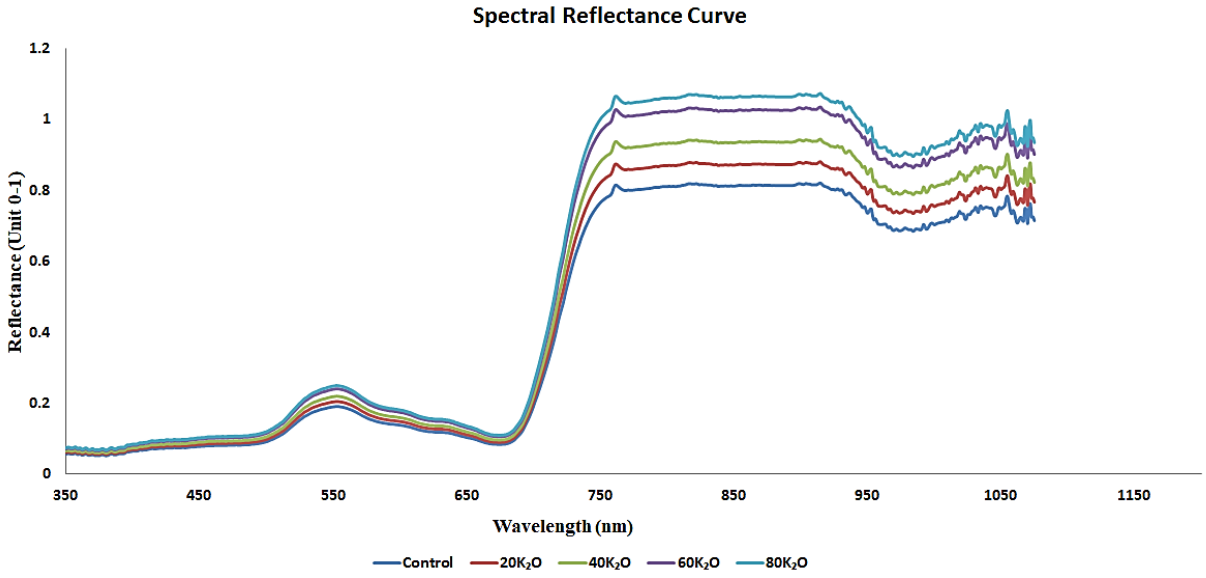


Figure 2. Mean spectral reflectance curves of sugar beet leaves under different potassium levels after 120 days from sowing.

3.1.2. ANOVA-based evaluation of spectral reflectance under potassium treatments

Figure 3 was used to statistically compare mean leaf reflectance among potassium treatments across the blue, green, red, and NIR spectral regions and to identify the spectral regions most responsive to K application.

One-way ANOVA showed that K application significantly affected leaf reflectance in the blue, green, red, and near-infrared spectral regions ($P < 0.05$; Figure 3). Mean reflectance generally increased with increasing K application rate, with 158.1 kg K ha^{-1} recording the highest numerical values in most spectral regions, followed by 118.6 kg K ha^{-1}, whereas the control recorded the lowest

values. Treatment separation was particularly evident in the NIR region, indicating K-related changes in internal leaf structure, canopy development, and biomass accumulation. However, the additional increase observed at 158.1 kg K ha^{-1} compared with 118.6 kg K ha^{-1} was relatively limited, suggesting diminishing optical gains at the highest K application rate. Thus, 118.6 kg K ha^{-1} provided a closely comparable and more balanced spectral response.

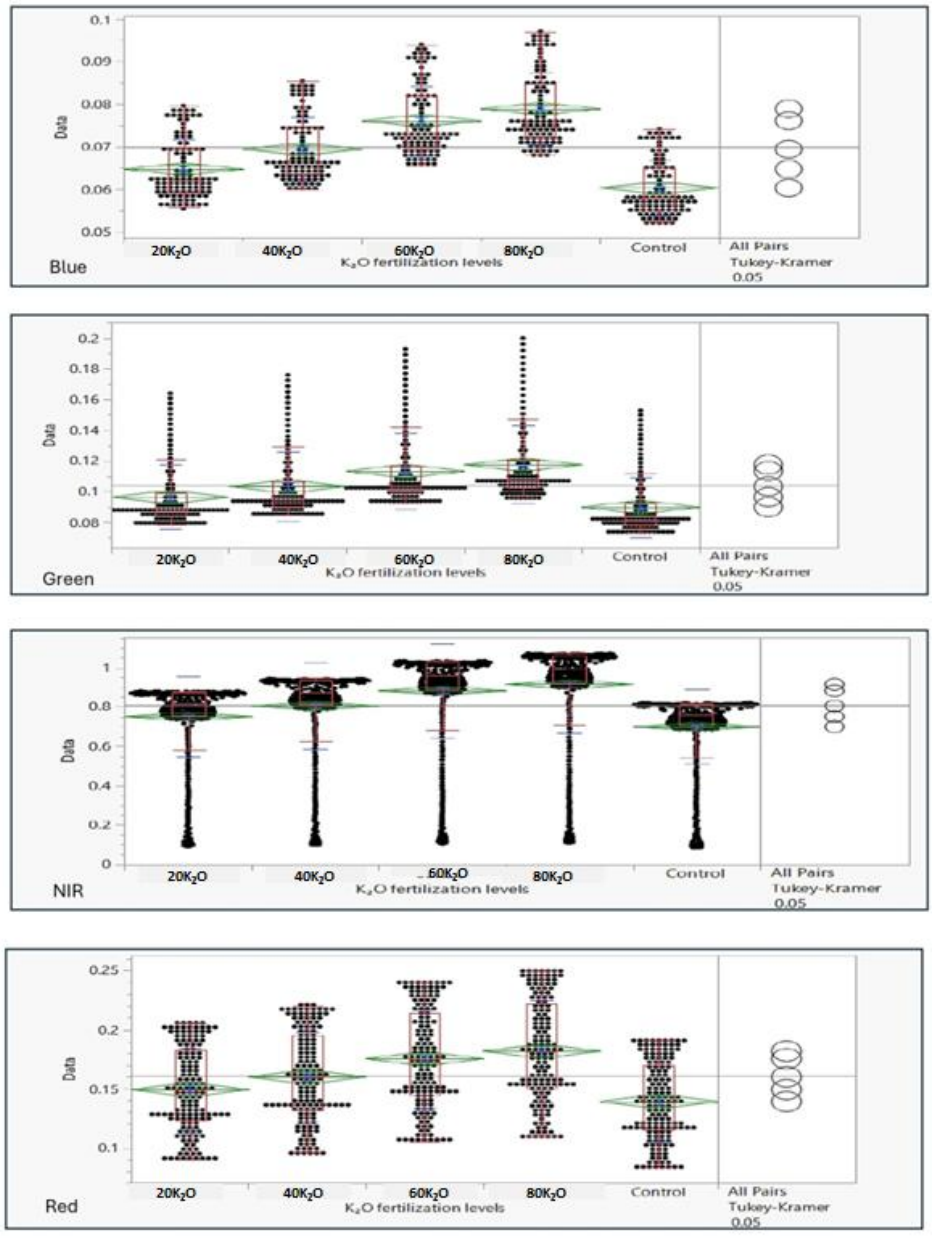


Figure 3. One-way ANOVA and Tukey–Kramer comparisons of sugar beet leaf reflectance in the blue, green, red, and NIR regions under different K application rates at 120 DAS.

The labels 20K$_2$O, 40K$_2$O, 60K$_2$O, and 80K$_2$O were retained as the original treatment codes and correspond to 39.5, 79.1, 118.6, and 158.1 kg K ha^{-1}, respectively.

3.1.3. Spectral vegetation indices at 120 DAS

Table 4 summarizes the variation in key spectral vegetation indices of sugar beet leaves under different potassium fertilization levels after 120 days from sowing. The Normalized Difference Vegetation Index (NDVI) showed slight but consistent improvement with potassium application, rising from 0.8027 in the control to 0.8075 at 79.1 kg K ha^{-1}, then stabilizing around 0.8057 at 158.1 kg K ha^{-1}. The Carotenoid Reflectance Index (CRI1) and Anthocyanin Reflectance Index (ARI1) revealed greater variation. While CRI1 remained relatively stable across treatments, ARI1 increased notably with higher potassium levels, peaking at 0.2962 under 158.1 kg K ha^{-1}, suggesting enhanced pigment content and reduced stress. PSRI values were negative across all treatments, with the lowest stress signature at the control (−0.0012) and most negative at 39.5 kg K ha^{-1} (−0.0182), implying subtle changes in senescence and leaf pigment balance. The Structure Insensitive Pigment Index (SIPI) increased steadily with potassium rate up to 118.6 kg K ha^{-1} (0.8215), then slightly decreased at 158.1 kg K ha^{-1}, indicating enhanced photosynthetic pigment stability. Overall, the spectral indices suggest that the 118.6 kg K ha^{-1} treatment provided optimal plant health and physiological balance, corroborating morphological and reflectance data trends.

Table 4. Spectral indices corresponding to sugar beet growth under potassium fertilization (120 DAS).

Treatment	NDVI	CRI1	ARI1	PSRI	SIPI
Control	0.8027	3.2501	0.5756	-0.0012	0.8128
39.5 kg K ha^{-1}	0.8048	3.2220	0.0588	-0.0182	0.8154
79.1 kg K ha^{-1}	0.8075	3.2570	0.1460	-0.0117	0.8187
118.6 kg K ha^{-1}	0.8038	3.1792	0.1874	-0.0073	0.8215
158.1 kg K ha^{-1}	0.8057	2.7753	0.2962	-0.0087	0.8102

Spectral vegetation indices were calculated mathematically from reflectance measurements and are presented as descriptive indicators.

3.2. Influence of potassium fertilization on chlorophyll content, shoot biomass, and root morphological traits

Table 5 presents complementary growth traits at 120 DAS, including SPAD value, shoot dry weight, and root diameter, whereas Table 3 reports root length, root fresh weight, and shoot fresh weight.

Table 5 outlines the influence of potassium fertilization on SPAD chlorophyll readings, shoot dry weight, and root diameter in sugar beet after 120 days from sowing over two growing seasons.

SPAD values, which estimate relative chlorophyll content, increased steadily with rising potassium application. In the 2024/2025 season, SPAD readings ranged from 40.70 in the control to 42.95 at 158.1 kg K ha^{-1}. Similarly, during the 2023/2024 season, values improved from 38.61 to 41.75. This trend reflects enhanced chlorophyll biosynthesis and photosynthetic efficiency under potassium supplementation.

In 2024/2025, shoot dry weight increased from 0.121 kg $plant^{-1}$ in the control to 0.177 kg $plant^{-1}$ at 158.1 kg K ha^{-1}. In 2023/2024, values increased from 0.081 to 0.131 kg $plant^{-1}$, indicating improved nutrient utilization and biomass accumulation with increasing K application rates.

Root diameter followed a similar pattern. It increased from 4.90 cm to 6.56 cm in 2024/2025 and from 5.30 cm to 6.45 cm in 2023/2024, indicating that potassium not only supports root elongation (Table 3) but also enhances radial development.

Within-season comparisons showed significant responses of root diameter, shoot dry weight, and SPAD to potassium fertilization. Between-season differences in shoot dry weight and SPAD were significant at all potassium rates. Root diameter differed significantly between seasons in the control and at 39.5 kg K ha^{-1}, whereas the differences at 79.1, 118.6, and 158.1 kg K ha^{-1} were not significant.

Table 5. Effect of potassium fertilization levels on growth sugar beet plants after 120 days from sowing.

K application rate (kg K ha^{-1})	Root diameter (cm) 2023/2024	2024/2025	Shoot dry weight (kg $plant^{-1}$) 2023/2024	2024/2025	SPAD 2023/2024	2024/2025
Control	5.30 d*	4.90 d*	0.081 c*	0.121 c*	38.61 e*	40.70 d*
39.5	5.80 c*	5.51 c*	0.100 bc*	0.142 bc*	39.95 d*	41.20 c*
79.1	6.03 b	5.92 b	0.105 b*	0.151 b*	40.40 c*	42.16 b*
118.6	6.33 a	6.45 a	0.112 ab*	0.163 ab*	41.42 b*	42.60 a*
158.1	6.45 a	6.56 a	0.131 a*	0.177 a*	41.75 a*	42.95 a*
LSD 5%	0.15	0.11	0.019	0.022	0.25	0.38

Means followed by different lowercase letters within the same season are significantly different according to the LSD test at $P \leq 0.05$. An asterisk (*) indicates a significant difference between the two growing seasons for the same potassium treatment at $P \leq 0.05$. Values without an asterisk are not significantly different between seasons.

3.2.1. Spectral reflectance at 120 DAS

Figure 4 illustrates the reflectance behavior of sugar beet leaves under different potassium fertilization levels after 120 days from sowing. Reflectance spectra were recorded between 350 and 1100 nm, showing clear differences among treatments.

In the visible region (400–700 nm), all treatments exhibited typical vegetation spectral patterns, including strong absorption near 450 nm and 680 nm and a reflectance peak around 550 nm, consistent with chlorophyll activity. In the near-infrared region (700–1100 nm), the 118.6 kg K ha^{-1} treatment displayed the highest reflectance, indicating improved internal leaf structure, cellular organization, and canopy development. The 39.5 and 79.1 kg K ha^{-1} treatments showed intermediate reflectance values, whereas the control consistently recorded the lowest values. The reflectance of the 158.1 kg K ha^{-1} treatment declined relative to that of the 118.6 kg K ha^{-1} treatment, particularly beyond 750 nm, indicating that increasing the K application rate above 118.6 kg K ha^{-1} did not provide an additional spectral benefit. Overall, the spectral profile supports 118.6 kg K ha^{-1} as the most balanced and efficient K application rate at 120 DAS.

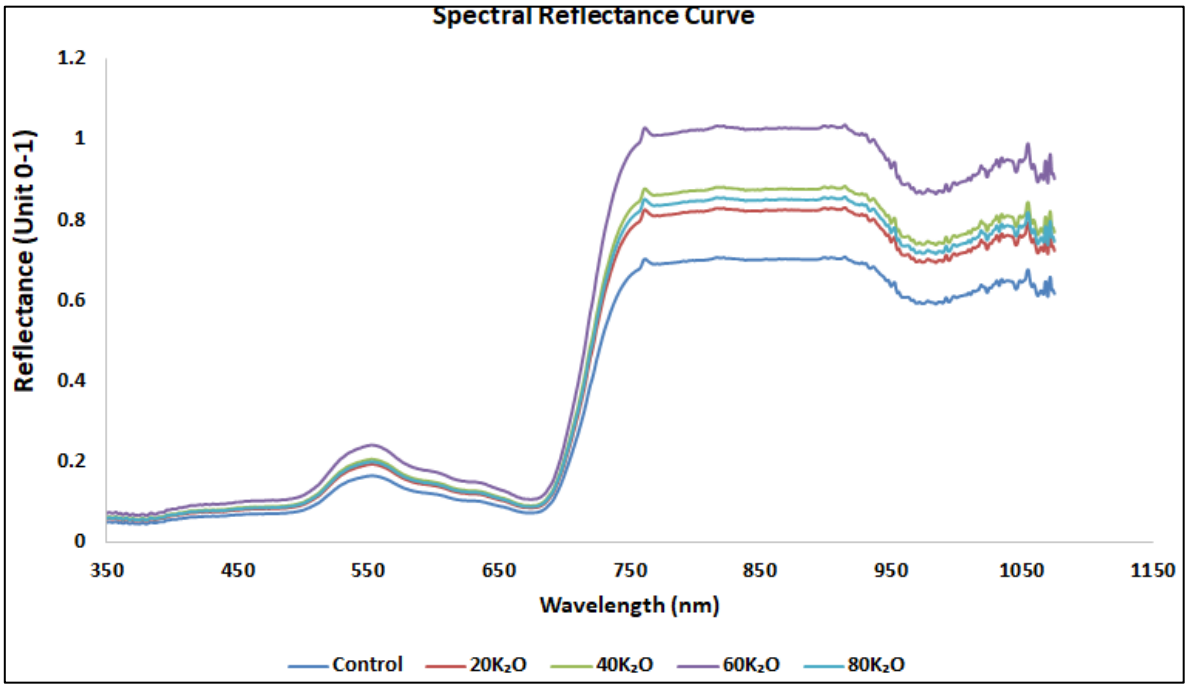


Figure 4. Mean spectral reflectance curves of sugar beet leaves under different K application rates at 120 DAS.

The labels $20K_2O$, $40K_2O$, $60K_2O$, and $80K_2O$ retained in the figure correspond to 39.5, 79.1, 118.6, and 158.1 kg K ha^{-1}, respectively.

3.2.2. One-way ANOVA of spectral reflectance at 120 DAS

Figure 5 was used to evaluate the statistical separation among potassium treatments across the main spectral regions at 120 DAS and to determine which spectral region was most sensitive to K application.

The ANOVA results revealed that potassium application had a significant effect on spectral reflectance across the studied wavelength regions ($P < 0.05$; Figure 5). Mean ± SE comparisons showed clear differences among treatments, with 118.6 kg K ha^{-1} producing the most favorable overall spectral response. In the blue and green regions, the control recorded the lowest reflectance values, whereas the 118.6 kg K ha^{-1} treatment showed higher values, indicating an improved canopy response. In the red region, the 118.6 kg K ha^{-1} treatment exhibited stronger chlorophyll-related absorption than the lower K rates. The clearest treatment separation occurred in the NIR region, where 118.6 kg K ha^{-1} produced the highest reflectance, indicating improved internal leaf structure, turgidity, and biomass accumulation. Moreover, increasing the K application rate to 158.1 kg K ha^{-1} did not provide an additional spectral benefit and resulted in slightly lower NIR reflectance than the 118.6 kg K ha^{-1} treatment. These findings support 118.6 kg K ha^{-1} as the most balanced and physiologically efficient K application rate at 120 DAS.

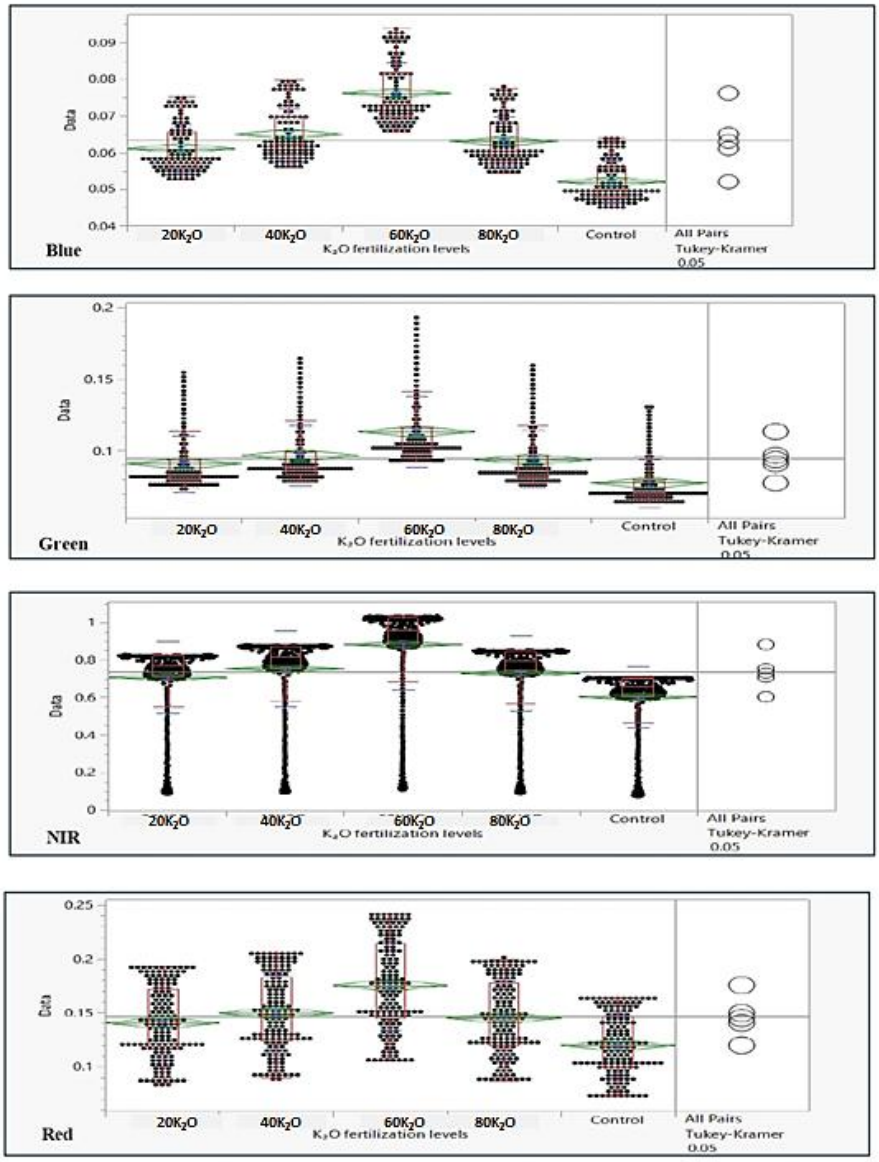


Figure 5. One-way ANOVA and Tukey–Kramer comparisons of sugar beet leaf reflectance in the blue, green, red, and NIR regions under different K application rates at 120 DAS.

The labels $20K_2O$, $40K_2O$, $60K_2O$, and $80K_2O$ are retained as the original treatment codes and correspond to 39.5, 79.1, 118.6, and 158.1 kg K ha^{-1}, respectively.

3.2.3. Spectral vegetation indices at 120 DAS (Root length & fresh biomass)

Table 6 illustrates the variation in spectral vegetation indices of sugar beet plants under different potassium fertilization levels after 120 days from sowing. The Normalized Difference Vegetation Index (NDVI) showed a slight increase across treatments, reaching its highest value of 0.8211 at 158.1 kg K ha^{-1}, indicating improved canopy vigor and greenness.

The Carotenoid Reflectance Index (CRI1) displayed notable variability, with the highest value (3.9571) recorded in the control and a significant reduction in 118.6 kg K ha^{-1} (2.9340), suggesting a shift in pigment composition under different K application rates. The Anthocyanin Reflectance Index (ARI1) peaked at 118.6 kg K ha^{-1} (0.3111), reflecting enhanced anthocyanin accumulation, possibly linked to moderate stress or metabolic regulation.

The Plant Senescence Reflectance Index (PSRI) showed consistently negative values, with the lowest (−0.0103) in the control and minimal variation among treatments, suggesting low senescence symptoms during sampling. The Structure Insensitive Pigment Index (SIPI) ranged from 0.8120 to 0.8283, with the highest value recorded under 158.1 kg K ha^{-1}, indicating increased carotenoid to chlorophyll ratios. Collectively, these results demonstrate that potassium application significantly influences spectral responses related to pigment composition and physiological status in sugar beet.

Table 6. Spectral indices corresponding to sugar beet growth under potassium fertilization (120 DAS).

Treatment	NDVI	CRI1	ARI1	PSRI	SIPI
Control	0.8125	3.9571	0.2467	−0.0103	0.8263
39.5 kg K ha^{-1}	0.7978	3.2098	0.2787	−0.0014	0.8120
79.1 kg K ha^{-1}	0.8100	3.7442	−0.1205	−0.0066	0.8232
118.6 kg K ha^{-1}	0.8129	2.9340	0.3111	−0.0068	0.8192
158.1 kg K ha^{-1}	0.8211	3.0454	0.1742	−0.0102	0.8283

Spectral vegetation indices were calculated mathematically from reflectance measurements and are presented as descriptive indicators.

3.3. Impact of potassium fertilization on final yield and root morphology

Table 7 presents the effect of potassium fertilization on sugar beet yield and root morphological characteristics at harvest during the 2023/2024 and 2024/2025 seasons.

Root yield significantly increased with rising potassium levels. In the 2024/2025 season, root yield improved from 6.511 kg m^{-2} in the control to a maximum of 7.185 kg m^{-2} at 158.1 kg K ha^{-1}. A similar trend was observed in 2023/2024, with yields increasing from 6.385 kg m^{-2} to 6.884 kg m^{-2}. This consistent enhancement indicates the pivotal role of potassium in promoting carbohydrate accumulation and root bulking. Root diameter showed substantial expansion in response to potassium addition. In the 2024/2025 season, diameter values increased from 11.71 cm (control) to 16.19 cm at the highest potassium dose, while the previous season followed a comparable trend, rising from 11.62 cm to 15.11 cm.

Likewise, root length increased with increasing K application rates, from 30.00 cm in the control to 32.07 cm at 158.1 kg K ha^{-1} in 2024/2025 and from 26.16 to 31.60 cm in 2023/2024.

Within each season, potassium fertilization resulted in significant differences in root length, root diameter, and root yield at harvest. Between-season comparisons showed significant differences in root yield at all potassium rates. Root length differed significantly between seasons from the control through 118.6 kg K ha^{-1}, whereas the difference at 158.1 kg K ha^{-1} was not significant. For root diameter, no significant difference between seasons was detected in the control, whereas significant differences occurred at all potassium-fertilized treatments.

Table 7. Effect of potassium fertilization levels on growth and yield sugar beet plants at harvest.

K application rate (kg K ha^{-1})	Root length (cm) 2023/2024	Root length (cm) 2024/2025	Root diameter (cm) 2023/2024	Root diameter (cm) 2024/2025	Root yield (kg m^{-2}) 2023/2024	Root yield (kg m^{-2}) 2024/2025
Control	26.16 e*	30.00 c*	11.62 d	11.71 d	6.385 d*	6.511 d*
39.5	27.59 d*	30.55 bc*	12.75 c*	13.63 c*	6.540 c*	6.750 c*
79.1	29.35 c*	31.27 ab*	13.80 b*	15.10 b*	6.742 b*	6.961 b*
118.6	30.55 b*	31.81 a*	14.63 a*	15.90 a*	6.831 a*	7.130 a*
158.1	31.60 a	32.07 a	15.11 a*	16.19 a*	6.884 a*	7.185 a*
LSD 5%	1.02	1.09	0.55	0.62	0.067	0.059

Means followed by different lowercase letters within the same season are significantly different according to the LSD test at $P \leq 0.05$. An asterisk (*) indicates a significant difference between the two growing seasons for the same potassium treatment at $P \leq 0.05$. Values without an asterisk are not significantly different between seasons.

3.3.1. Spectral reflectance at growth and harvest

In Figure 6, spectral reflectance curves of sugar beet leaves under different potassium fertilization levels showed overall similarity in shape across the 350–1100 nm range, with the typical vegetation pattern of absorption troughs near 450 nm (blue) and 680 nm (red), and a reflectance peak around 550 nm (green).

In the red edge and near-infrared region (700–900 nm), all treatments exhibited a sharp increase in reflectance, though with relatively close values. The control consistently recorded the lowest reflectance, reflecting reduced chlorophyll content and weaker canopy development. Treatments with 79.1 kg K ha^{-1} and 118.6 kg K ha^{-1} showed slightly higher reflectance than the control and 39.5 kg K ha^{-1}, suggesting improved leaf structure and physiological activity.

Although differences among treatments were not very pronounced, the moderate potassium application rates (79.1–118.6 kg K ha^{-1}) tended to enhance NIR reflectance compared to the control and the higher rate (158.1 kg K ha^{-1}), which showed no additional gain. These spectral responses align with the expected role of potassium in supporting leaf biomass and canopy density.

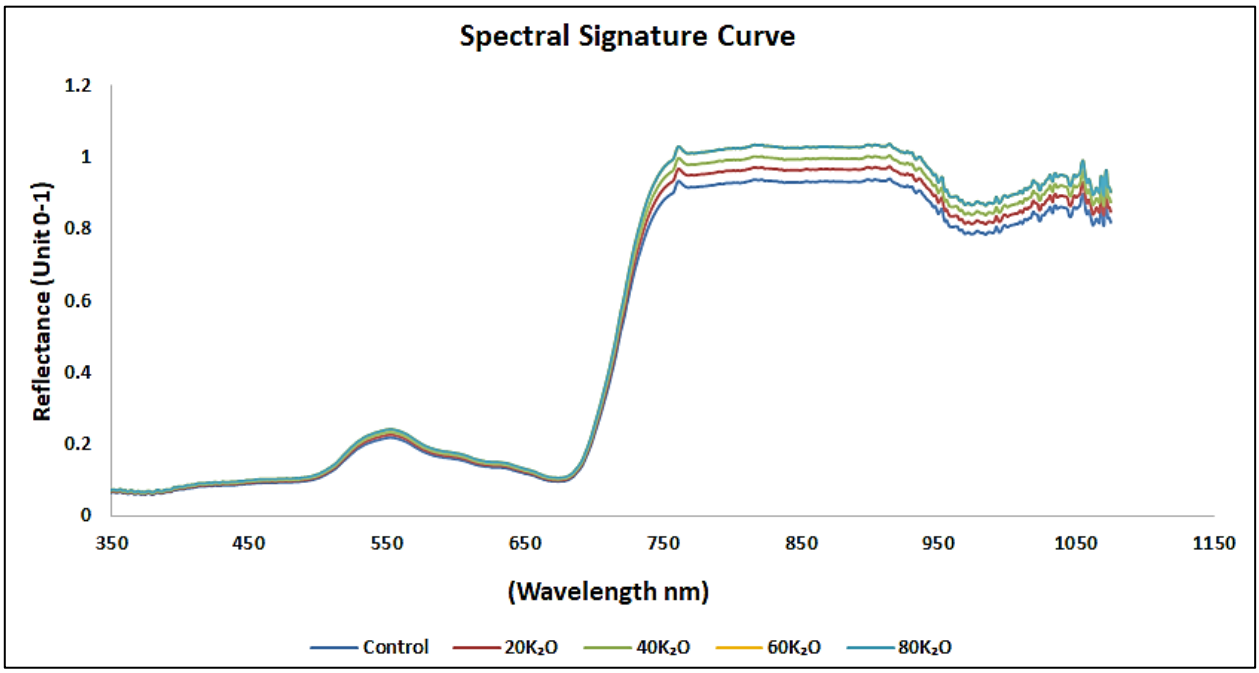


Figure 6. Mean spectral reflectance curves of sugar beet leaves under different potassium fertilization levels at harvest stage.

3.3.2. One-way ANOVA of spectral reflectance at growth and harvest

Figure 7 was used to assess whether the spectral differences among potassium treatments persisted until harvest and to identify the spectral regions that remained most responsive to K application at 180 DAS.

At harvest, one-way ANOVA confirmed that K application significantly influenced sugar beet leaf reflectance in the blue, green, red, and NIR regions ($P < 0.05$; Figure 7). The 118.6 and 158.1 kg K ha^{-1} treatments generally produced the highest and closely comparable reflectance values, whereas the control recorded the lowest values. The relatively overlapping treatment distributions and Tukey–Kramer comparisons indicate that the differences among the higher K rates were less pronounced at harvest than at 120 DAS. The NIR region continued to show the clearest response to adequate K nutrition, reflecting improved internal leaf structure and canopy development. Because 158.1 kg K ha^{-1} provided no clear additional optical advantage over 118.6 kg K ha^{-1}, the latter was considered the more efficient and balanced application rate under the experimental conditions.

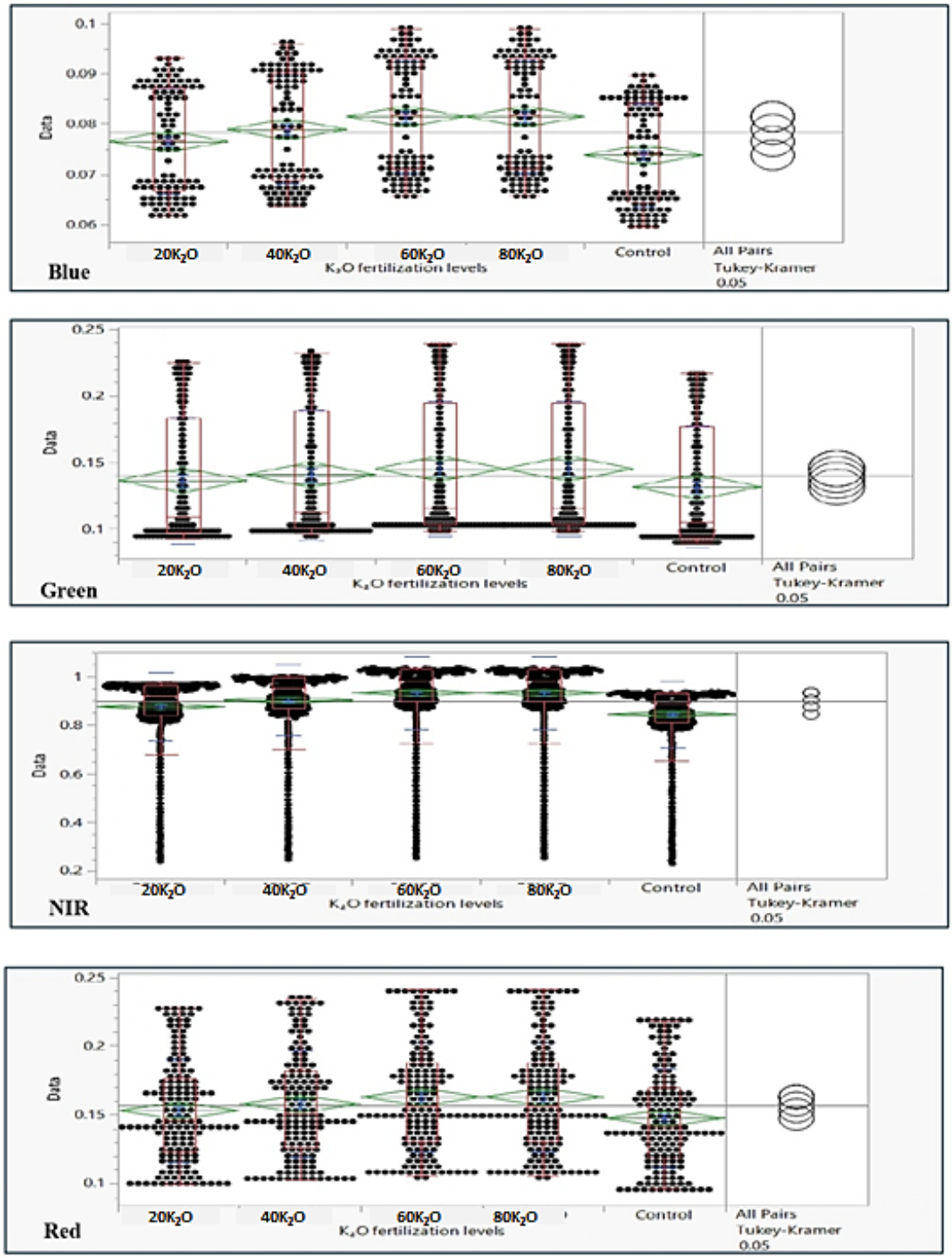


Figure 7. One-way ANOVA and Tukey–Kramer comparisons of sugar beet leaf reflectance in the blue, green, red, and NIR regions under different K application rates at harvest (180 DAS).

The labels $20K_2O$, $40K_2O$, $60K_2O$, and $80K_2O$ are retained as the original treatment codes and correspond to 39.5, 79.1, 118.6, and 158.1 kg K ha^{-1}, respectively.

3.3.3. Spectral vegetation indices at growth and harvest

Table 8 illustrates the variation in key spectral vegetation indices among sugar beet plants treated with different potassium levels. The Normalized Difference Vegetation Index (NDVI) showed a slight increase across treatments, reaching its highest value of 0.8211 at 158.1 kg K ha^{-1}, indicating improved canopy vigor and greenness. The Carotenoid Reflectance Index (CRI1) showed fluctuating trends, peaking at 3.9346 under 39.5 kg K ha^{-1}, then declining to 3.1174 at 118.6 kg K ha^{-1}. This may reflect changes in carotenoid accumulation or pigment degradation under higher nutrient levels. The Anthocyanin Reflectance Index ARI1 ranged from −0.0236 at 39.5 kg K ha^{-1} to 0.2909 in the control. Among the K-fertilized treatments, the highest ARI1 value was recorded at 118.6 kg K ha^{-1} (0.2600). Interestingly, the ARI1 was negative at 39.5 kg K ha^{-1} (−0.0236), indicating lower pigment stress under low potassium.

PSRI values remained negative across all treatments, with minimal variation, indicating consistent chlorophyll stability. SIPI values ranged from 0.8136 to 0.8200, with the highest value recorded at 79.1 kg K ha^{-1}, reflecting improved pigment ratios and potential photosynthetic efficiency.

These spectral indices highlight subtle physiological and biochemical responses of sugar beet to potassium application, with 118.6 kg K ha^{-1} and 158.1 kg K ha^{-1} showing optimal spectral signatures.

Table 8. Effect of potassium fertilization on spectral vegetation indices of sugar beet plants at harvest.

Treatment	NDVI	CRI1	ARI1	PSRI	SIPI
Control	0.8043	3.7972	0.2909	−0.0061	0.8171
39.5 kg K ha^{-1}	0.8116	3.9346	−0.0236	−0.0117	0.8163
79.1 kg K ha^{-1}	0.8091	3.7259	0.1634	−0.0063	0.8200
118.6 kg K ha^{-1}	0.8040	3.1174	0.2600	−0.0098	0.8136
158.1 kg K ha^{-1}	0.8125	3.2832	0.2351	−0.0090	0.8186

Spectral vegetation indices were calculated mathematically from reflectance measurements and are presented as descriptive indicators.

Additional exploratory analyses describing within-treatment variability among individual plants and soil samples at 118.6 kg K ha^{-1} are provided in the Supplementary Material (Figures S1–S4; Tables S1).

4. Discussion

Potassium fertilization had a marked and consistently positive effect on sugar beet morphology and canopy physiology under the sandy soils of Nubaria. Across two seasons, increasing K application rates progressively enhanced root and shoot growth at 120 DAS, with the most pronounced and stable improvements observed at 118.6–158.1 kg K ha^{-1}. This pattern agrees with the well-established roles of potassium in maintaining cellular turgor, activating metabolic enzymes, enhancing assimilate translocation, and regulating osmotic balance, all of which collectively support vegetative expansion and biomass accumulation [43]. The associated increase in SPAD values and the enlargement of root diameter under higher K rates confirm enhanced chlorophyll synthesis and improved radial root development [44], which agrees with earlier findings reporting improved sugar beet growth and quality traits under adequate potassium nutrition [45]. Studies further emphasize that potassium

supplementation improves root structural integrity, chlorophyll stability, and carbon allocation efficiency, particularly in arid and nutrient-limited systems [46].

The vegetation spectral signature defined as the characteristic pattern of reflectance across the visible and near-infrared regions offers a powerful, non-destructive indicator of plant physiological and biochemical status. These signatures provide direct information about chlorophyll concentration, nutrient availability, and leaf water status [47,48]. Variations in reflectance, especially shifts in the red and blue absorption troughs, the green peak, and the red-edge slope, are widely recognized as sensitive markers of pigment composition, canopy structure, and physiological stress conditions [49,50].

Advances in hyperspectral research have further demonstrated that subtle changes in reflectance at narrow wavebands can detect nutrient imbalances, early stress responses, and alterations in mesophyll structure long before visible symptoms appear [49].

Building upon these physiological trends, the hyperspectral results provide deeper mechanistic interpretation of plant responses to potassium availability. The characteristic vegetation reflectance curve, marked by strong absorption in the blue and red wavelengths, a green reflectance peak, and a pronounced red-edge transition, was consistently observed across treatments, yet its magnitude shifted in direct association with K application rate. Such shifts are well-documented indicators of chlorophyll density, mesophyll structure, and canopy vigor [47,48,50,51].

Moderate potassium supply (approximately 118.6 kg K ha^{-1}) generated the most physiologically coherent spectral response: Deeper absorption in the VIS range, sharper red-edge slope, and elevated NIR reflectance, collectively signifying enhanced pigment concentration, more efficient photosynthetic machinery, and better-developed leaf internal structure. This trend aligns with findings that optimal K fertilization enhances canopy spectral behavior through improved chloroplast integrity, stomatal conductance, and tissue hydration [52].

The superior spectral performance observed under 118.6 kg K ha^{-1} suggests that this fertilization level optimized physiological functioning without inducing excessive nutrient accumulation. In contrast, the absence of proportional improvements at 158.1 kg K ha^{-1} indicates diminishing returns under higher potassium supply, emphasizing the importance of balancing nutrient inputs to maximize nutrient-use efficiency and sustainability.

Conversely, the highest K application rate (158.1 kg K ha^{-1}) often exhibited elevated NIR reflectance without proportional VIS improvements, indicating possible nutrient imbalance or early physiological stress. The relatively limited improvement observed at 158.1 kg K ha^{-1} compared with 118.6 kg K ha^{-1} may indicate a saturation response under the experimental conditions. This response could be associated with luxury potassium consumption, whereby plants absorb potassium in excess of their physiological requirements without achieving proportional improvements in growth or productivity. Similar observations have been reported under high potassium availability, where additional potassium uptake resulted in limited agronomic benefits and reduced potassium-use efficiency [52]. This pattern, characterized by elevated NIR reflectance without proportional improvement in visible-region absorption, has been associated with excessive nutrient application and saturation effects in hyperspectral crop studies, particularly under intensive fertilization regimes [49].

At harvest, potassium fertilization continued to exert advantages on yield formation and root morphological traits; however, the spectral responses consistently pointed to moderate K (≈118.6 kg K ha^{-1}) as the physiologically efficient rate. Although the 158.1 kg K ha^{-1} treatment sometimes produced the highest numerical yield values, its spectral behavior, particularly in the VIS and NIR domains, did not reflect proportional functional improvements relative to 118.6 kg K ha^{-1}. This phenomenon aligns

with hyperspectral studies showing that excessive K supply often enhances structural reflectance (NIR) without corresponding gains in pigment absorption or metabolic efficiency [53,54]. The convergence of optical and agronomic indicators thus supports approximately 118.6 kg K ha^{-1} as the practical optimum under sandy soil conditions, capturing most of the physiological and yield benefits while avoiding the diminishing returns and subtle stress signals associated with over-fertilization. Vegetation indices derived from hyperspectral reflectance are widely recognized as robust indicators of plant physiological status, pigment composition, and canopy structure under varying nutrient conditions. Such indices have been successfully applied to characterize crop vigor, stress responses, and biochemical variability in a range of agricultural systems [1,36,40,51]. Their spectral responses can also be influenced by variations in plant nutrient status and environmental conditions [55–57]. These findings are also consistent with established spectral interpretations of nutrient sufficiency and excess [52]. Together, these patterns demonstrate that hyperspectral sensing can simultaneously capture the stabilizing effect of potassium nutrition and subtle plant- or soil-level deviations, reinforcing its value for precision nutrient monitoring.

Collectively, the results highlight three practical points. First, potassium nutrition in sandy soils yields consistent agronomic gains that are detectable non-destructively through hyperspectral measurements. Second, the convergence of morphological, spectral, and index-based evidence around 118.6 kg K ha^{-1} provides a defensible, economically efficient target rate for comparable environments, while higher doses risk diminishing physiological returns. Third, while within-treatment spectral differences among plants and soils exist, these are manageable sources of variation rather than confounders; when acknowledged and controlled, they can even offer diagnostic value for singling out atypical plants or microsites [58]. These findings suggest that hyperspectral indicators are sensitive not only to nutrient sufficiency but also to the physiological consequences of excessive fertilization, providing a valuable tool for identifying nutrient-use efficiency thresholds under sandy soil conditions.

These findings agree with advances in crop spectral diagnostics showing that optimized potassium supply enhances canopy biochemical status and red-edge behavior while preventing stress-related increases in reflectance variability [57]. Moreover, the strengthening of NIR signals under adequate K input aligns with current physiological models describing the relationship between nutrient status and mesophyll structure**.**

From a sustainability standpoint, the integration of field spectroscopy with standard agronomy offers an actionable path toward precision nutrient management in resource-limited, sandy landscapes. By aligning fertilizer rates with plant-level physiological signals, producers can avoid over-application, conserve inputs, and stabilize yield formation. These outcomes support sustainable crop production without over-extending claims beyond the agronomic scope of this study.

Our findings highlight important implications for sustainable crop production. The enhanced productivity observed under sandy soil conditions demonstrates how precision fertilization can maximize output in marginal lands. This may contribute to improving the productivity of sugar beet, an important industrial and food crop, under sandy soil conditions. By reducing the risks of nutrient deficiency and over-fertilization, such practices support more resilient and resource-efficient production systems under climate and resource constraints. This work not only contributes to optimizing potassium fertilization in sugar beet but also aligns with broader strategies for sustainable nutrient management and resource-use efficiency in arid environments. Collectively, these outcomes are consistent with sustainability frameworks emphasizing nutrient-use efficiency, spectral monitoring, and climate-resilient agronomy [5].

5. Study limitations

This study was conducted at a single experimental site under sandy soil conditions in Egypt, which may limit the generalization of the findings to other environments. Root quality parameters such as sucrose concentration, juice purity, and sugar content were not evaluated and therefore could not be integrated into the assessment of potassium fertilization responses. In addition, direct quantitative correlations between vegetation indices and agronomic traits were not performed. In future studies, researchers should include multi-location trials and integrate root quality measurements with spectral analyses to strengthen the applicability of hyperspectral approaches for potassium management in sugar beet production systems.

6. Conclusions

This study highlights the significant role of potassium fertilization in enhancing sugar beet (*Beta vulgaris L.*) growth performance, productivity, and spectral reflectance characteristics under sandy soil conditions. The integration of hyperspectral remote sensing with vegetation indices provided an effective, non-destructive framework for monitoring plant responses to nutrient management.

Among the tested treatments, 118.6 kg K ha^{-1} provided the most balanced agronomic, physiological, and spectral response. Although the highest numerical root yield and several morphological values were recorded at 158.1 kg K ha^{-1}, the differences from 118.6 kg K ha^{-1} were limited, while the spectral responses indicated no proportional additional benefit from the highest K rate. Therefore, 118.6 kg K ha^{-1} may represent an efficient potassium management rate under the experimental conditions. Statistical analyses (ANOVA) verified the significant influence of potassium fertilization on spectral reflectance behavior and vegetation indices, supporting the reliability of hyperspectral indicators for evaluating crop nutritional status. Spectral indices such as NDVI, CRI1, SIPI, ARI1, and PSRI proved sensitive to potassium availability and effectively reflected changes in pigment composition, biomass accumulation, and plant physiological condition. The observed consistency between spectral parameters and agronomic traits underscores the value of hyperspectral sensing as a precise diagnostic tool for crop monitoring and fertilizer optimization. Beyond agronomic benefits, optimizing potassium fertilization through hyperspectral-based monitoring represents a practical approach to precision agriculture in arid and resource-limited environments. Such strategies enhance productivity, reduce the risk of nutrient over-application, and contribute to sustainable crop production systems aligned with sustainable crop production and improved nutrient management under sandy soil conditions. Overall, the findings provide strong evidence that 118.6 kg K ha^{-1} may represent an effective potassium management strategy for balancing growth, physiological performance, and sustainability in sugar beet cultivation under sandy soil conditions. This work advances our understanding of nutrient–spectral relationships and supports the development of more resilient and resource-efficient agricultural practices.

Use of AI tools declaration

The authors declare they have not used Artificial Intelligence (AI) tools in the creation of this article.

Acknowledgments

The authors would thank the National Authority of Remote Sensing and Space Science (NARSS) -Cairo, Egypt, the National Research Center and RUDN University as this publication has been supported by the RUDN University Scientific Projects Grant System project no. 202786-2-000.

Conflict of interest

The authors declare that there is no any conflict of interest.

Author contributions

Ghada A. Khdery: Conceptualization, Methodology, Investigation, Formal analysis, Data curation, Software, Visualization, Writing–original draft, Writing–review & editing, Validation, Project administration. I. M. El-Metwally: Methodology, Investigation, Resources, Writing–review & editing, Supervision. Nazih Y. Rebouh: Formal analysis, Writing–review & editing, Visualization. Oybek Fayziev: Software, Writing–review & editing. Mohamed S. Shokr: Investigation, Data curation, Formal analysis, Writing–review & editing.

References

1. El-Metwally IM, El-Shahawy TAE (2025) Enhancing sugar beet quality and productivity under the effects of co-application of urea and herbicides on weed control and crop performance. *Bull Natl Res Cent* 49: 36. https://doi.org/10.1186/s42269-025-01327-1
2. Brar NS, Dhillon BS, Saini K, et al.(2015) Agronomy of sugarbeet cultivation-A review. *Agric Rev* 36: 184–197. https://doi.org/10.5958/0976-0741.2015.00022.7
3. Wimmer S, Sauer J (2020) Profitability development and resource reallocation: The case of sugar beet farming in Germany. *J Agric Econ* 71: 816–837. https://doi.org/10.1111/1477-9552.12373
4. Tayyab M, Wakeel A, Mubarak MU, et al. (2023) Sugar beet cultivation in the tropics and subtropics: challenges and opportunities. *Agronomy* 3: 1213. https://doi.org/10.3390/agronomy13051213
5. FAO (2022) FAOSTAT: Food and Agriculture Organization of the United Nations. Available from: https://www.fao.org/faostat/en/#data.
6. Statista (2023) Leading sugar beet producers worldwide by production volume. Available from: https://www.statista.com/statistics/264670/top-sugar-beet-producers-worldwide-by-volume/.
7. Bairagi A, Paul SK, Kader MA, et al. (2013) Yield of tropical sugarbeet as influenced by variety and rate of fertilizer application. *Pak Sugar J* 28: 13–20.
8. Paul S, Paul U, Sarkar MAR, et al. (2018) Yield and quality of tropical sugarbeet as influenced by variety, spacing and fertilizer application. *Sugar Tech* 20: 175–181. https://doi.org/10.1007/s12355-017-0545-3
9. Elbeih SF (2021) Evaluation of agricultural expansion areas in the Egyptian deserts: A review using remote sensing and GIS. *Egypt J Remote Sens Space Sci* 24: 889–906. https://doi.org/10.1016/j.ejrs.2021.10.004

10. Draycott AP, Christenson DR (2003) *Nutrients for sugar beet production: Soil-plant relationships*. Wallingford, UK: CABI Publishing. https://doi.org/10.1079/9780851996233.0000
11. Johnson RT, Alexander JT, Rush GE, et al. (1971) *Advances in sugarbeet production: principles and practices*. Ames, Iowa: The Iowa State University Press, 470 pp.
12. Wang M, Zheng Q, Shen Q, et al. (2013) The critical role of potassium in plant stress response. *Int J Mol Sci* 14: 7370–7390. https://doi.org/10.3390/ijms14047370
13. Ghahremani A, Akbari K, Yousefpour M, et al. (2014) Effects of nano-potassium and nano-calcium chelated fertilizers on qualitative and quantitative characteristics of Ocimum basilicum. *Int J Pharm Res Sch* 3: 235–241.
14. Zangeneh N, Rasouli M (2017) Effect of potassium fertilizers and humic acid on the pigments and activity of antioxidants in grape'Bidaneh Sefid'. *Iran J Hortic Sci* 48: 701–714. https://doi.org/10.22059/ijhs.2017.229264.1202
15. Abdallah MMS, El-Bassiouny HMS, AbouSeeda MA (2019) Potential role of kaolin or potassium sulfate as anti-transpirant on improving physiological, biochemical aspects and yield of wheat plants under different watering regimes. *Bull Natl Res Cent* 43: 134. https://doi.org/10.1186/s42269-019-0177-8
16. Jasim AH, Sura R, Hanaa MJ (2020) Effect of skip irrigation and nano potassium treatments on maize yield. *Ecol Environ Conserv* 26: 963–968.
17. Hermans C, Hammond JP, White PJ, et al. (2006) How do plants respond to nutrient shortage by biomass allocation? *Trends Plant Sci* 11: 610–617. https://doi.org/10.1016/j.tplants.2006.10.007
18. Amer M, Attalah M, Ibrahim MF, et al. (2004) Effect of potassium fertilizer on mineral contents and some biological components of ten sugar beet varieties. *J Agric Sci Mansoura Univ* 29: 2963–2978.
19. Efe R, Ekinci D, Cürebal İ (2008) Erosion analysis of Findikli creek catchment (NW of Turkey) using GIS based on RUSLE (3D) method. *Fresenius Environ Bull* 17: 568–576.
20. Tilling AK, O'Leary GJ, Ferwerda JG (2007) Remote sensing of nitrogen and water stress in wheat. *Field Crops Res* 104: 77–85. https://doi.org/10.1016/j.fcr.2007.03.023
21. Feng W, Zhu Y, Tian YC, et al. (2008) Monitoring leaf nitrogen accumulation in wheat with hyper-spectral remote sensing. *Acta Ecol Sin* 28: 23–32. https://doi.org/10.1016/S1872-2032(08)60018-9
22. Meggio F, Zarco-Tejada PJ, Núñez LC, et al. (2010) Grape quality assessment in vineyards affected by iron deficiency chlorosis using narrow-band physiological remote sensing indices. *Remote Sens Environ* 114: 1968–1986. https://doi.org/10.1016/j.rse.2010.04.004
23. Ramoelo A, Dzikiti S, Van Deventer H, et al. (2015) Potential to monitor plant stress using remote sensing tools. *J Arid Environ* 113: 134–144. https://doi.org/10.1016/j.jaridenv.2014.09.003
24. Caturegli L, Grossi N, Saltari M, et al. (2015) Spectral reflectance of tall fescue (Festuca Arundinacea Schreb.) under different irrigation and nitrogen conditions. *Agric Agric Sci Procedia* 4: 59–67. https://doi.org/10.1016/j.aaspro.2015.03.008
25. Karaburun A (2009) Estimating potential erosion risks in Corlu using the GIS-based RUSLE method. *Fresenius Environ Bull* 18: 1692–1700.
26. Argyrokastritis IG, Papastylianou P, Alexandris S (2015) Leaf water potential and crop water stress index variation for full and deficit irrigated cotton in Mediterranean conditions. *Agric Agric Sci Procedia* 4: 463–470. https://doi.org/10.1016/j.aaspro.2015.03.054

27. Katsoulas N, Elvanidi A, Ferentinos KP, et al. (2016) Crop reflectance monitoring as a tool for water stress detection in greenhouses: A review. *Biosyst Eng* 151: 374–398. https://doi.org/10.1016/j.biosystemseng.2016.10.003
28. Wang L, Zhou X, Zhu X, et al. (2017) Estimation of leaf nitrogen concentration in wheat using the MK-SVR algorithm and satellite remote sensing data. *Comput Electron Agric* 140: 327–337. https://doi.org/10.1016/j.compag.2017.05.023
29. Hongo C, Niwa K, Yokobori J, et al. (2009) Development of an efficient sugar beet cultivation support system using the agricultural spatial information—Prediction of root yield using meteorological data and satellite data. *Proc 35th Biennial Meet Am Soc Sugar Beet Technol*: 490.
30. Clevers JGPW (1997) A simplified approach for yield prediction of sugar beet based on optical remote sensing data. *Remote Sens Environ* 61: 221–228. https://doi.org/10.1016/S0034-4257(97)00004-7
31. Yones M, Ma'moun SA, Farag RMA, et al. (2019) Hyperspectral application for early diagnosis of American foulbrood disease in the honeybee (Apis mellifera L.) larvae. *Egypt J Remote Sens Space Sci* 22: 271–277. https://doi.org/10.1016/j.ejrs.2019.05.002
32. Wang Q, Shao K, Cai Z, et al. (2025) Prediction of sugar beet yield and quality parameters using Stacked-LSTM model with pre-harvest UAV time series data and meteorological factors. *Artif Intell Agric* 15: 252–265. https://doi.org/10.1016/j.aiia.2025.02.004
33. Asaka D (1995) The use of LANDSAT TM data for estimating the interaction of sugar beet yields damaged by cold and wet weather in 1993 with soil properties. *J Jpn Soc Soil Phys* 72: 27–37. https://doi.org/10.34467/jssoilphysics.72.0_27
34. Guerif M, Duke C (1998) Calibration of the SUCROS emergence and early growth module for sugar beet using optical remote sensing data assimilation. *Eur J Agron* 9: 127–136. https://doi.org/10.1016/S1161-0301(98)00031-8
35. Launay M, Guerif M (2005) Assimilating remote sensing data into a crop model to improve predictive performance for spatial applications. *Agric Ecosyst Environ* 111: 321–339. https://doi.org/10.1016/j.agee.2005.06.005
36. Merzlyak MN, Gitelson AA, Chivkunova OB, et al. (1999) Non-destructive optical detection of pigment changes during leaf senescence and fruit ripening. *Physiol Plant* 106: 135–141. https://doi.org/10.1034/j.1399-3054.1999.106119.x
37. Xu L, Myneni RB, Chapin FS, et al. (2013) Temperature and vegetation seasonality diminishment over northern lands. *Nat Clim Change* 3: 581–586.
38. Rouse JW Jr, Haas RH, Deering DW, et al. (1974) *Monitoring the vernal advancement and retrogradation (green wave effect) of natural vegetation,* College Station, TX: Remote Sensing Center, Texas A&M University, Final Report RSC-1978-4, NASA-CR-144661.
39. Mascarini L, Lorenzo GA, Vilella FJ (2006) Leaf area index, water index, and red: Far red ratio calculated by spectral reflectance and its relation to plant architecture and cut rose production. *J Am Soc Hortic Sci* 131: 313–319. https://doi.org/10.21273/JASHS.131.3.313
40. Gitelson AA, Merzlyak MN, Chivkunova OB (2001) Optical properties and nondestructive estimation of anthocyanin content in plant leaves. *Photochem Photobiol* 74: 38–45. https://doi.org/10.1562/0031-8655(2001)074%3C0038:OPANEO%3E2.0.CO;2

41. Gitelson AA, Stark R, Grits U, et al. (2002) Vegetation and soil lines in visible spectral space: A concept and technique for remote estimation of vegetation fraction. *Int J Remote Sens* 23: 2537–2562. https://doi.org/10.1080/01431160110107806
42. Huete A, Jackson RD (1988) Soil and atmosphere influences on the spectra of partial canopies. *Remote Sens Environ* 25: 89–105. https://doi.org/10.1016/0034-4257(88)90043-0
43. Cakmak I (2005) The role of potassium in alleviating detrimental effects of abiotic stresses in plants. *J Plant Nutr Soil Sci* 168: 521–530. https://doi.org/10.1002/jpln.200420485
44. Marschner P (2012) *Marschner's mineral nutrition of higher plants*. 3rd ed. Academic press. https://doi.org/10.1016/C2009-0-63043-9
45. Zörb C, Senbayram M, Peiter E (2014) Potassium in agriculture–status and perspectives. *J Plant Physiol* 171: 656–669. https://doi.org/10.1016/j.jplph.2013.08.008
46. Gomaa M, Abdel-Nasser G, Maareg MF, et al. (2017) Sugar Beet Response to Nitrogen and Potassium Fertilization Treatments in Sandy Soil. *J Adv Agric Res* 22: 272–287. https://doi.org/10.21608/jalexu.2017.278510
47. Khdery GA, Farg E, Arafat SM (2019). Natural vegetation cover analysis in Wadi Hagul, Egypt using hyperspectral remote sensing approach. *T Egypt J Remote Sens Space Sci* 22: 253–262. https://doi.org/10.1016/j.ejrs.2019.09.002
48. Khdery G, Gad AA, El-Zeiny AM (2020) Spectroscopic characterization of plant cover in El-Fayoum Governorate, Egypt. *Egypt J Soil Sci* 60: 397–408. https://doi.org/10.21608/ejss.2020.36730.1377
49. Furlanetto RH, Crusiol LGT, Nanni MR, et al. (2024) Hyperspectral data for early identification and classification of potassium deficiency in soybean plants (Glycine max (L.) Merrill). *Remote Sens* 16: 1900. https://doi.org/10.3390/rs16111900
50. Khdery G, Yones M (2021) Innovative spectral library for identification common wild plants using hyperspectral technology in Northwestern Coast, Egypt. *Egypt J Remote Sens Space Sci* 24: 485–491. https://doi.org/10.1016/j.ejrs.2020.08.002
51. Khdery GA, Shokr MS, Rebouh NY, et al. (2025) Spectral and morphological discrimination of Ficus and Moringa species with medical and nutritional relevance: Toward sustainable plant utilization. *Front Sustain Food Syst* 9: 1652332. https://doi.org/10.3389/fsufs.2025.1652332
52. Sidhu SK, Zotarelli L, Sharma LK (2024) A review of potassium significance and management approaches in potato production under sandy soils. *J Sustain Agric Environ* 3: e12106. https://doi.org/10.1002/sae2.12106
53. Gitelson AA, Buschmann C, Lichtenthaler HK (1999) The chlorophyll fluorescence ratio F735/F700 as an accurate measure of the chlorophyll content in plants. *Remote Sens Environ* 69: 296–302. https://doi.org/10.1016/S0034-4257(99)00023-1
54. Clevers JGPW, Kooistra L (2012) Using hyperspectral remote sensing data for retrieving canopy chlorophyll and nitrogen content. *IEEE J Sel Top Appl Earth Obs Remote Sens* 5: 574–583. https://doi.org/10.1109/JSTARS.2011.2176468
55. Li H, Liu F, Zhang X, et al. (2024) Magnesium deficiency or excess hinders tomato growth, potassium and calcium uptake. *Plant Soil Environ* 70: 719–730. https://doi.org/10.17221/473/2023-PSE

56. Miranda M, Sun X, Marín A (2022) Nano-and micro-sized carnauba wax emulsions-based coatings incorporated with ginger essential oil and hydroxypropyl methylcellulose on papaya: Preservation of quality and delay of post-harvest fruit decay. *Food Chem X* 13: 100249. https://doi.org/10.1016/j.fochx.2022.100249
57. Lobell DB, Asner GP (2002) Moisture effects on soil reflectance. *S Soil Sci Soc Am J* 66: 722–727. https://doi.org/10.2136/sssaj2002.7220
58. Stenberg B, Rossel RAV, Mouazen AM, et al. (2010) Visible and near infrared spectroscopy in soil science. *Adv Agron* 107: 163–215.



© 2026 the Author(s), licensee AIMS Press. This is an open access article distributed under the terms of the Creative Commons Attribution License (https://creativecommons.org/licenses/by/4.0)